Unified Studies of Fast-Ignition Scheme Fusion with Counterbeam Configuration

Y. Kitagawa[1], Y. Mori[1], K. Ishii[1], R. Hanayama[1], Y. Nishimura[1], S. Nakayama[1], T. Sekine[2], T. Kurita[2], N. Satoh[2], T. Kawashima[2], H. Kan[2], O. Komeda[3], T. Nishi[3], T. Hioki[4], T. Motohiro[4], H. Azuma[5], A. Sunahara[6], Y. Sentoku[7], E. Miura[8], Y. Arikawa[9], Y. Abe[9], and S. Ozaki[10]

[1]*Graduate School for the Creation of New Photonics Industries, Hamamatsu, Shizuoka, Japan*
[2]*Hamamatsu Photonics, K.K., Hamamatsu City, Shizuoka, Japan*
[3]*TOYOTA Central R&D Labs Inc., Nagakute, Aichi, Japan*
[4]*Green Mobility Collaborative Research Center (GREMO), Nagoya University, Nagoya, Japan*
[5]*Aichi Synchrotron Radiation Center, Seto-shi, Aichi-ken, 489-0965 Japan*
[6]*Institute for Laser Technology, Suita, Osaka, Japan*
[7]*University of Nevada, Reno, NV 89557, USA*
[8]*National Institute of Advanced Industrial Science and Technology (AIST), Tokyo, Japan*
[9]*Institute of Laser Engineering, Osaka University, Osaka, Japan*
[10]*National Institute for Fusion Science (NIFS), Toki, Gifu, Japan*
Corresponding Author: Y. Kitagawa, kitagawa@gpi.ac.jp

The recent key physics of the laser fusion is how to make hot sparks for the alpha burning in the dense core. The fast ignition is expected to form a hot spark even with a nonuniform illumination configuration, such as with a counter-illumination one. By using both a high-repetition rate 10 J laser and a single-shot kJ laser, we have proposed and demonstrated a new concept for the fast-ignition scheme fusion, where main beams implode a shell target with counterbeam configuration and ultraintense lasers with the same configuration drive either hot electrons or ions or both, which has directly heated the core. Shock waves driven by ultraintense lasers are also powerful candidates for the core heating and are investigated. Combining these three fast-ignition schemes, we are demonstrating both the implosion and ignition to work well with counterbeam configuration.

Published as a journal article in Nuclear Fusion
http://iopscience.iop.org/article/10.1088/1741-4326/aa70bc

Unified Studies of Fast-ignition Scheme Fusion with Counterbeam Configuration

Y. Kitagawa[1], Y. Mori[1], K. Ishii[1], R. Hanayama[1], Y. Nishimura[1,2], S. Okihara[1], S. Nakayama[1], T. Sekine[3], M. Takagi[3], T. Watari[3], N. Satoh[3], T. Kawashima[3], H. Kan[3], O. Komeda[4], T. Hioki[5], T. Motohiro[5], H. Azuma[6], A. Sunahara[7], Y. Sentoku[8], Y. Arikawa[8], T. Nagai[8], Y. Abe[8], E. Miura[9] and S. Ozaki[10]

[1]The Graduate School for the Creation of New Photonics Industries, Hamamatsu, Japan
[2]Toyota Technical Development Corporation, Toyota Aichi Japan
[3]Hamamatsu Photonics, K. K., Hamamatsu Japan
[4]Advanced Material Engineering Division, TOYOTA Motor Corporation, Susono, Shizuoka Japan
[5]Materials Science and Energy Eng. Division, Green Mobility Research Institute, Institutes of Innovation for Future Society, Nagoya University
[6]Aichi Synchrotron Radiation Center In *Knowledge Hub Aichi*, Seto, Aichi Japan
[7]Institute for Laser Technology, Osaka Japan
[8]Institute of laser Engineering, Osaka University
[9]National Institute of Advanced Industrial Science and Technology, Tsukuba, Ibaraki Japan
[10]National Institute for Fusion Science, Toki, Gifu Japan

Corresponding Author: kitagawa@gpi.ac.jp

Abstract:
The recent key physics of the laser fusion is how to make hot sparks for the alpha burning in the dense core. The fast ignition is expected to form a hot spark even with a non-uniform illumination configuration, such as with a counter-illumination one. By using both a high-repetition rate 10 J laser and a single-shot kJ laser, we have proposed and demonstrated a new concept for the fast-ignition scheme fusion, where main beams implode a shell target with counterbeam configuration and ultraintense lasers with the same configuration drive either hot electrons or ions or both, which has directly heated the core. Shock waves driven by ultraintense lasers are also powerful candidates for the core heating and are investigated. Combining these three fast-ignition schemes, we are demonstrating both the implosion and ignition to work well with counterbeam configuration.

1 Introduction

Because of its structural simplicity, inertial confinement fusion (ICF) stands close to the breakeven and high gain points. It, nevertheless, has many issues to be solved. High-density compression and core heating are essential processes for the inertial confinement

fusion, and it requires that we solve the issue of core heating for the ignition.A self ignition scheme, that is, to burn the core in implosion itself has not proved as easy as expected. A promising solution for this is the fast-ignition scheme.

In the fast-ignition scenario of ICF, a DD or DT capsule is preimploded and is irradiated with a laser pulse for a few tens of picoseconds, which is much shorter than the hydrodynamic disassembly time of the compressed core [1]. Such a short-pulse laser generates energetic electrons and ions near the cutoff region. These electrons and ions are expected to penetrate into the core and form a hot spot. From the hot spot, an ^3He (α particle) burning wave spreads over the core. The fast heating and ignition will powerfully help the inertial confinement fusion to produce energy, if it succeeds in triggering the core ignition with high gain.

In previous fast heating studies, a petawatt laser [2] enhanced the neutron yields to the order of 10^6 n/4π sr [3]. However, 2D simulations and experiments suggest that the hot electrons diverge, thereby heating the whole core area rather than a local region [4, 5, 6, 7, 8, 9].

We propose a scheme that directly heats imploded cores by energetic ions driven by an ultraintense laser LFEX. The laser drives both hot electrons and energetic ions around the critical density. Fractions of these driven particles are transported through the overdense plasma to the core. Hot electrons will heat the whole core, while energetic ions will deposit their large amount close to the core periphery, locally heating it to the ^{4}He (α particle) burning temperature. An α burning wave then spreads from the hot spot over the core. A spherical deuterated polystyrene (C_8D_8 or CD) shell was polarily imploded by two counterbeams of a GEKKO XII (GXII) green laser. LFEX is focused onto the naked core from the side, vertical to the GXII axis. Illuminating LFEX to the core as close as possible shows us that both the hot electrons and energetic ions play main roles in core heating. In fact, DD beam-fusion neutrons with the yield of 5×10^8 n/4π sr are observed.

2 Target with heating holes and counter beams implosion

The self-ignition scheme fusion requires a 4π laser beam illumination, because it needs to concentrate centrifugal shock waves to make a central hot spark. But the fast-ignition scheme may not require such a fully symmetrical illumination, because the fast ignition beam can form a hot spark in any core area.

The diameter and thickness of the target are 7 and 500 μm, respectively [as shown in Fig. 2(c)]. The target has two 250-μm diameter holes, one to guide the LFEX beam into the target and the other to ventilate the preplasmas generated by GXII. The latter hole is not for heating, but enables direct detection of x-rays and charged particles emitted from the heated core. As in Figs. 1, by changing the focusing depth of the counter implosion beams, we have investigated the focal point to have the highest core density. Each of the two counterbeams from GXII carries 254 ± 14 J in a 1.3-ns-wide Gaussian pulse at

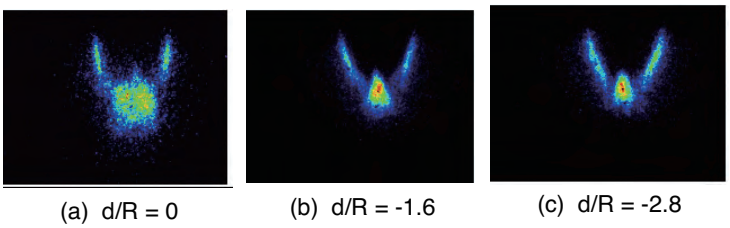

FIG. 1: Radius-time flow diagrams of the shells at focal depth of (a) $d/R = 0, I = 3.7 \times 10^{15}\, W/cm^2, Ny = 5 \times 10^5/4\pi\, sr$ *(b)* $d/R = -1.6, I = 1.5 \times 10^{15}\, W/cm^2, Ny = 1.9 \times 10^5/4\pi\, sr$ *and (c)* $d/R = -2.8, I = 9.7 \times 10^{14}\, W/cm^2, Ny = 1 \times 10^5/4\pi\, sr$. *$R$ is shell radius, I is laser intensity on target surface, and Ny is neutron yield.*

a wavelength of $0.527\,\mu$m. Figure 1 (b) shows us the best focal point point to be at $400\,\mu$m over the center, that is, $d/R = -1.6$, where we have DD thermal neutron yield of 1.9×10^5 and a 1-dimensional hydro code STAR1D estimated the peak density to be around $5 \sim 10\times$the solid density. The results show the counter beam configuration (F number 3) can implode a spherical shell to form a dense quasi-spherical core. Since the

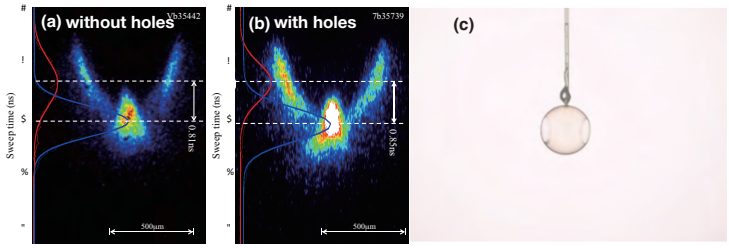

FIG. 2: Comparison of x-ray streak flows between (a) a simple shell target without holes and (b) a shell used here with side holes.(c) CD shell with two holes for LFEX introduction and for preplasma ventilation. Horizontal axis: 1 ns/div, vertical axis: $250\,\mu m/div$*(Hamamatsu Photonics C4575-03).*

side holes are perpendicular to the GXII laser axis and of the same size as the spots ($\sim 250\,\mu$m), the two laser spot area and the two hole areas are so small as 20 % of the whole shell area, respectively, that they will not affect two-beam implosion. We have compared x-ray streak flow images for similar shell targets without and with side holes in Figs. 2(a) and (b), respectively. The results show no apparent differences. The intensities of the core emission were the same.

3 LFEX and measurement setup

Figure 3(a) is an imaginary moment of lFEX illumination onto the core. Un imploded areas of the shell remain. Figure 3(b) shows the configuration of the target, lasers, and detectors. An aspheric lens (F number 3) focuses each beam of two counterbeams of GXII onto position $d/R = -1.6$. The intensity of the beam on the target is $3.1 \times 10^{14}\,\mathrm{W/cm^2}$. The cross section of the LFEX beam is $80\,\mathrm{cm} \times 40\,\mathrm{cm}$. An off-axial parabolic mirror with

a focal length of 4 m (F number 10) focuses 50 % of 613 J LFEX in 1.5 ps at a wavelength of 1.053 μm onto a 60-μm-diameter spot, producing an intensity of 1×10^{19} W/cm^2 in vacuum. The LFEX and GXII beams are electronically synchronized (jitter $<$ 100 ps).

Figure 3(c) shows the core emission without LFEX illumination. The bottom plot represents the imploding shell emission trajectory, which follows the GXII pulse shape. One dimensional hydrocode, STAR 1D [10], predicts the maximum compression of the core 0.9 ns after the implosion beam peak, while XSC shows in Fig. 3(c) that the emission peak is 0.8 ns, probably due to the hot electron or shock preheating.

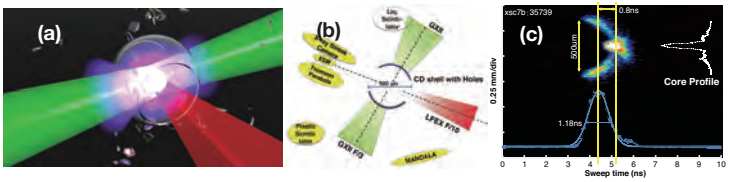

FIG. 3: (a) CD shell counterimploded by two GXII beams and a 79° side heated by LFEX. (b) Arrangements of the target, lasers, and detectors. (c) Same target as Fig. 2(b).

4 X-ray Pinhole images of LFEX-heated Cores

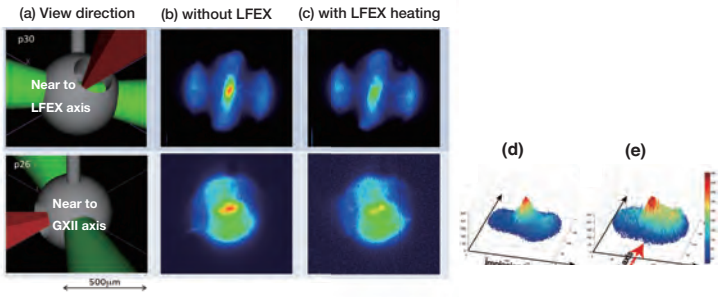

FIG. 4: (a) Upper picture indicates the view direction of x-ray pinhole camera near to the LFEX axis, and lower is near to the GXII axis, respectively. (b) Pinhole images of shell without LFEX and (c) those with LFEX. (d) 3D image from lower (b) without LFEX. (e) 3D image from lower (c) with LFEX.

Figure 4(a) upper and lower images indicate the view directions of two pinhole cameras, respectively. (b) displays the x-ray pinhole images of the target in the 2-3 keV energy range without LFEX beam. (c) are images with LFEX beam. The emission size is 360 μm FWHM along the GXII beam, while it is 230 μm along the LFEX axis; therefore, the LFEX absorption point is 0.6 times closer to the core than expected in a uniform implosion. Note that the peak core emission without LFEX seems brighter than that with LFEX. Observed emissions from the heated core are reduced, which may be due to that the heated emissions become higher and shift out of the observation range of 2-3 keV.

Lower (b) and (c) are reconstructed to 3 dimensiional images in (d) and (e), respectively. As indicated by an arrow in (e), LFEX is illuminated at the time of peak core

emission. The core diameter is $55\pm1\,\mu$m in full width at half maximum (FWHM). Assuming that the imploding beams converge two $(200\times200\times7)\,\mu m^3$ shell volumes into a 55-μm-wide and 230-μm-long ellipsoidal core, the material is compressed to at least twice its solid density ($2\,g/cm^3$). Although STAR 1D predicts the $5-10\,g/cm^3$ compression of the core, the narrow width of the beam cone angle (19°) realizes only twice the solid density under 2D expansion. STAR 1D estimated also that the core radius and temperature at the maximum compression are 35 μm and ~0.8 keV, respectively.

5 Neutrons

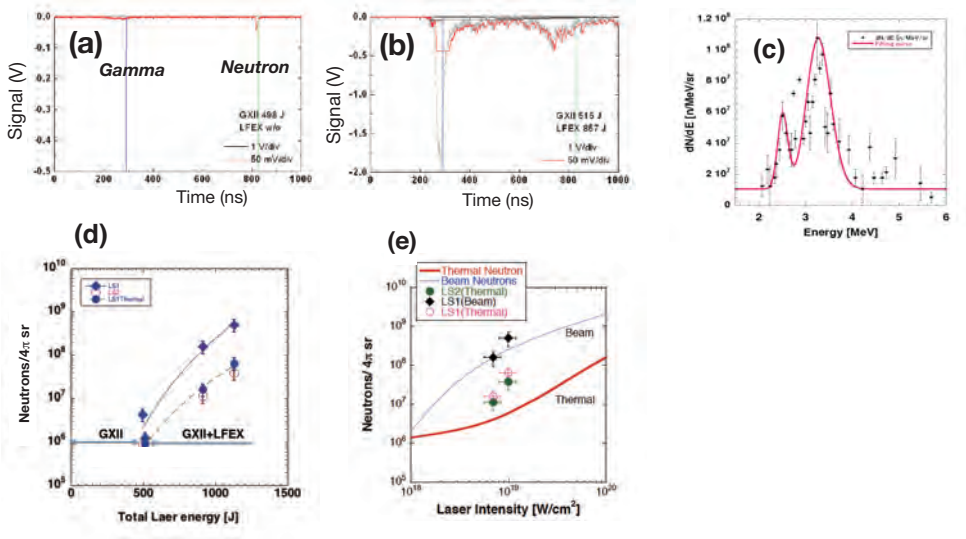

FIG. 5: (a) Neutron and γ TOF signals from LS1 : Shot No. 35739 of 498-J GXII without LFEX : the neutron yield is $7\times10^5/4\pi$ sr, and (b) Shot No. 35732 of 515-J GXII + 613-J LFEX. (c) Neutron energy spectrum, converted from (b). Small peak at 2.45 MeV is a thermal peak with a yield of 6.4×10^7 $n/4\pi$ sr. Large peak is a beam-fusion peak with 5×10^8 $n/4\pi$ sr. (d) Neutrons from LS1 (thermal: solid circles; beam: diamonds) and LS2 (thermal+beam: open circles) versus GXII+LFEX laser energy E. The instrumental and calibration error is 32%. The dashed line is proportional to E^5. (e) STAR 1D: beam fusion and thermal fusion yields versus LFEX intensity on the target. Solid lines are the beam- and dotted are thermal-fusion, respectively. Diamonds and circles are the experiments in (f).

The neutron time-of-flight (TOF) signals were detected by two gated oxygen-enriched liquid scintillators [11]. Liquid scintillator LS1 was set 13.35 m from the target at 69.13°(right-forward) to the LFEX incidence (in the horizontal direction); Liquid scintillator LS2 was set 2.5 m from the target perpendicular to the LFEX axis. To prevent γ noises, we electronically gated the photomultiplier dynode prior to the arrival of the neutron signals. Before illuminating LFEX, we confirmed that the neutrons were generated from the core and not from the shell. The yield without LFEX was 10^5-10^6 n/4π sr/shot: LS2 detected 7×10^5 (No. 35739). The TOF signals from LS1 without LFEX are shown in Fig. 5(a).

Illumination by both GXII and LFEX shows a large DD neutron yield (the TOF signal and its energy spectrum are shown in Figs. 5(b) and (c), respectively). The solid angle and sensitivity of LS1 are 1.4×10^{-4} sr and 1 count/5.6 neutrons, respectively.

As in Fig. 5(c), the neutron signals in (b) were fitted by a two-peak Gaussian curve: $dN/dE = 1{\times}10^7{+}9.8{\times}10^7 \exp -[(\sqrt{E}{-}\sqrt{3.3})^2/0.01]{+}4.9{\times}10^7 \exp -[(\sqrt{E}{-}\sqrt{2.5})^2/0.0025]$, where the energy unit is MeV. The second term on the right-hand side describes the main peak in Fig. 5(c), which is up-shifted from 2.45 to 3.3 MeV. Although LS1 was angled $-69.13°$ (right-forward) from the LFEX axis, we infer that the peak at 3.3 MeV arises from beam fusion (width ΔE_B is 0.01 MeV$\times \ln 2$=6.9 keV at HWHM). The third term describes the peak at 2.5 MeV (width ΔE_T is 0.0025 MeV$\times \ln 2$=1.7 keV at HWHM), and is inferred as the core temperature. Integrating the curve from 2 to 6 MeV and normalizing by 4π sr, we obtain the yield of $(5.1 \pm 1.6) \times 10^8$ n/4π sr. The peak at 2.5 MeV corresponds to 6.4×10^7 n/4π sr (13% of the total yield), indicating that thermal neutrons have been enhanced 100-fold from 5×10^5 n/4π sr and that the core temperature has roughly doubled from 0.8 to 1.8 keV. From the Planck relation, the x-ray pinhole emission of 2−5 keV infers the core temperature to be 0.8−2 keV [12]. The total yield normalized by 4π sr is $3.8{\times}10^7$ n/4π sr, of the same order as the 2.45 MeV peak yield in the LS1 signal [Fig. 5(c)].

In Fig. 5(d) the 4π angle neutron yields from LS1 and LS2 are plotted as functions of the total laser energy E (LFEX+GXII). No LFEX is illuminated up to 500 J. The solid circles indicate the neutrons yielded by thermal fusion at around 2.45 MeV. The dashed line in Fig. 5(e) is proportional to E^5 and represents the best fit to the experimental data. Assuming that the core temperature T_c is proportional to E and the thermal yield is proportional to T_c^5, an increase from 500 J to 1.1 kJ corresponds to a T_c increase from 0.8 to 1.8 keV, raising the yield from 5×10^5 to 2.5×10^7 n/4π sr.

The neutron yields were confirmed by STAR 1D assuming 50% absorption by the hot electrons with the 4-MeV-slope temperature and 1.3 % conversion to carbon^{+6} and deuteron^{+1} at a laser intensity of 1×10^{19} W/cm^2. The temperatures of the bulk electrons and of the ions are 1.8 keV close to the surface and 1.0 keV far from the surface, respectively. Figure 5(e) plots the STAR 1D lines as functions of the LFEX intensity. Deuterons and carbons are related to beam fusion and thermal fusion lines, respectively. The diamonds and solid circles are the experimental points in Fig. 5(d).

6 Ion and electron emissions from the core

We positioned two CR-39 ion-track detectors (a) at 20.9° and (b) 109° relative to the LFEX incidence. The signals detected at (a) have traveled straight throughout the core and are shown in Fig. 6(a); the side signals detected at (b) are shown in Fig. 6(b). Both detectors are positioned 10 cm from the target. The counting areas of both detectors is 0.0227 mm^2, implying a detection solid angle of 2.3×10^{-6} sr. Before LFEX arrives at the target, the GXII illumination ablates and removes the surface hydrocontamination layers. Therefore, LFEX heats pure CD plasma, producing only hot electrons, energetic carbons and deuterons.

Deuterons of Fig. 6(a) are rarely observed below 1 MeV, comparing with those of (b).

The deuterons generated at the cutoff density must include energies from below 1 MeV to above a few tens MeV[13]. As suggested in Fig. 4(d), these deuterons must be emitted over broad solid angles. Therefore, those coming from the core, Fig. 6(a), must be stopped. Figure 6(b) seems to show that the side scattered ones are not stopped. Their nonexponential decay must be the result of capturing additional deuterons, pulled by runaway hot electrons, which explains the large count difference between the signals (a) and (b) [71 counts of Fig. 6(a) versus 231 counts of Fig. 6(b)]. An electron spectrometer placed on the LFEX axis detected hot electrons throughout the core with a 5.5-MeV-slope temperature as shown in 6(c). The lack energy below $\sim$ 13 MeV seems to be absorbed in the core.

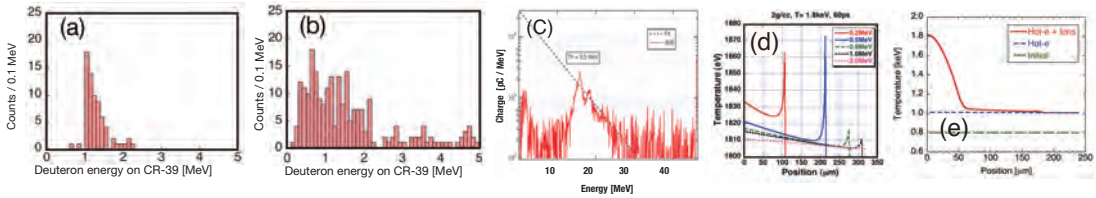

FIG. 6: (a) Ion spectrum of shot No. 35737 from CR-39 track Detector-a. 71 counts are detected. (b) Spectrum from Detector-b. 231 counts are detected. Detectors comprise a 20-μm-thick aluminum filter and three stacks of 100-μm-thick CR-39 films. (c) Electron energy spectrum to LFEX front direction. (d) STAR 1D temperature profile of CD plasma, heated by slowdown of the injected fast deuterons. The initial energy of the deuterons is 0.2, 0.5, 0.8, 1.0 and 2.0 MeV. (e) STAR 1D simulations: 50 % absorption of hot electrons heats the core to 1 keV. Fast carbons heat the core surface from 1 to 1.8 keV. Core surface is at 0 and center at 240 μm.

From the 2D rad-hydro calculations, the peak density and size of the core plasma were determined as 2 g/cm^3 and 230 μm, respectively. Using these values, we calculated the deuteron stopping range in fully ionized CD plasmas at various initial energies and are plotted in Fig. 6(d). Deuterons of 0.9 MeV or less are stopped by the 230 μm core, consistent with the results of Fig. 6(a). According to the STAR 1D [see Fig. 6(d)], hot electrons heat the entire core from 800 eV to 1 keV, whereas carbon^{+6} predominantly heats the region 20 μm from the core surface from 1 to 1.8 keV. The thermal- and beam-fusion yields are 2.3×10^7 and 4.1×10^8 n/4π sr, respectively, consistent with observations. Although the beam fusion neutrons were not uniformly distributed over all solid angles, we estimated the 4π sr yield for comparison with the 1D simulations.

Particle-in-cell (PIC) simulations predict that hot electrons spread over $\sim 60^\circ$. The present path to the core area, however, is so short (100 μm), that more than a third (33%) of the hot electrons strike the core plasma and deposit their energy [3].

7 Conclusion

The preimploded core of the CD shell target was heated by direct illumination of LFEX, yielding 5×10^8 DD neutrons by deuteron-beam fusion. This result verifies that the core

is locally heated by ions. Thermonuclear neutrons are driven by energetic ions such as carbon^{+6}. STAR 1D results reasonably agreed with the experiments. LFEX increased the core temperature from 0.8 to 1.8 keV locally on its periphery. PICLS coupled to STAR 1D could evaluate the bulk heating and heat transport mechanism by the LFEX driven electrons and ions. Our polar implosion scheme achieves the advantage of ion heating by placing the ignition laser closer to the core than in spherical implosion schemes. A part of this manuscript is published in [14].

This study was conducted under the collaborative program of the Institute of Laser Engineering (ILE), Osaka University. Authors wishing to acknowledge the LFEX and GXII operation, measurement, and target fabrication from the ILE team. We also thank H. Azechi, Y. Sakawa and H. Nishimura of ILE for contributions to this study.

References

[1] M. Tabak *et al.*, *Phys. Plasmas* **1**,1626 (1994).

[2] Y. Kitagawa *et al.*, *IEEE J. Quantum Electron.* **40**, 281 (2004).

[3] Y. Kitagawa *et al.*, *Phys. Rev. E* **71**, 016403 (2005).

[4] S. Atzeni, J. Meyer-ter-Vehn, *The Physics for Inertial Fusion, Beam Plasma Interaction, Hydrodynamics, Hot Dense Matter* (Oxford Science Publications, New York, 2004).

[5] Y. Sentoku *et al.*, *Phys. Plasmas* **11**, 3083 (2004).

[6] R. Jung *et al.*, *Phys. Rev. Lett.* **94**, 195001 (2005).

[7] A. L. Lei *et al.*, *Phys. Rev. Lett.* **96**, 255006 (2006).

[8] N. Naumova *et al.*, *Phys. Rev. Lett.* **102**, 025002 (2009).

[9] Y. Kitagawa *et al.*, *Phys. Rev. Lett.* **108**, 155001 (2012).

[10] A. Sunahara *et al.*, Plasma Fusion Res. **3**, 043 (2008).

[11] Y. Arikawa *et al.*, *Rev. Sci. Instrum.* **83**, 10D909 (2012).

[12] Ya. B. Zel'dovich and Yu. P. Raizer, *Physics of Shock Waves and High-temperature Hydrodynamic Phenomena*, (Academic Press, New York, 1967), Vol.I, p.116.

[13] S. C. Wilks, and W. L. Kruer, *IEEE J. Quantum Electron.* **33**, 1964 (1997).

[14] Y. Kitagawa *et al.*, *Phys. Rev. Lett.* **114**, 195002 (2015).

[15] Y. Sentoku, and A. J. Kemp, *J. Comput. Phys.* **227**, 6846 (2008).